



Article

Research on Trajectory Tracking Control of a Semi-Trailer Train Based on Differential Braking

Wencong Wang , Gang Li * and Shuwei Liu

School of Automobile and Traffic Engineering, Liaoning University of Technology, Jinzhou 121001, China; 219904013@stu.lnut.edu.cn (W.W.); lgqclsw@lnut.edu.cn (S.L.)

* Correspondence: qcxyiligang@lnut.edu.cn

Abstract: How to improve the driving performance of the vehicle while carrying out path tracking control has become a hot issue in current research. In this paper, an MPC (Model predictive control) path tracking control algorithm incorporating differential braking control is proposed. By establishing a vehicle dynamics model of a semi-trailer train, the model predictive control theory is adopted for path tracking. Then, the vehicle dynamics model, considering the additional yaw moment, is established to design the differential braking control strategy. Under low-speed working conditions, the PID (Proportional Integral Derivative) algorithm is used to solve the additional yaw moment with the yaw rate of the tractor traveling alone as the desired value. Under high-speed working conditions, the Fuzzy PID algorithm is used to solve the additional yaw moment with the control objective of reducing the articulation angle. Simulation models are built using MATLAB/Simulink, and TruckSim for numerical experimental validation. The numerical experimental results show that the differential braking control method proposed in this paper can improve the maneuverability of vehicles driving in low-speed conditions and the stability of vehicles driving in high-speed conditions without decreasing the precision of path tracking control.

Keywords: trajectory tracking control; model predictive control; differential braking; semi-trailer train



Citation: Wang, W.; Li, G.; Liu, S. Research on Trajectory Tracking Control of a Semi-Trailer Train Based on Differential Braking. *World Electr. Veh. J.* **2024**, *15*, 30. <https://doi.org/10.3390/wevj15010030>

Academic Editor: Joeri Van Mierlo

Received: 11 December 2023

Revised: 4 January 2024

Accepted: 5 January 2024

Published: 16 January 2024



Copyright: © 2024 by the authors. Licensee MDPI, Basel, Switzerland. This article is an open access article distributed under the terms and conditions of the Creative Commons Attribution (CC BY) license (<https://creativecommons.org/licenses/by/4.0/>).

1. Introduction

Applying automatic driving technology to semi-trailer trains significantly improves driving safety, enhances traffic flow efficiency [1], and optimizes logistics costs. Automated driving technology mainly includes four significant parts: perception, positioning [2], planning, and control, of which the trajectory tracking control module is to solve the problem of how the vehicle travels by the planned path, which is the critical link to realizing automatic driving of the car [3]. Compared with the general single car, a semi-trailer train has a large turning radius and is difficult to pass in the narrow channel [4]. When driving at high speed, it is likely to occur side-slip, tailing, folding, and other dangerous conditions, increasing the difficulty of semi-trailer train trajectory tracking control.

Many scholars have carried out much research on semi-trailer train travel control. In their paper, Changfu Zong et al. [5] propose a multi-objective followability control algorithm based on differential braking for preventing rollovers or folds in semi-trailer trains. It can improve the vehicle's stability during transient maneuvering and prevent the car from dangerous working conditions such as rollover and folding. Zhe Leng et al. [6] used active speed limiting to improve the steering characteristics and solve the steering limitation problem. An extended Kalman filter sideslip estimator is designed to achieve sideslip compensation. Both algorithms can work directly with other control algorithms to improve the accuracy of vehicle trajectory tracking on curved roads. The trajectory tracking control error was reduced by Ming Yue et al. [7]. A model predictive control method is used to design the attitude controller, and a global terminal slip film control method is used to create the dynamic controller. The error in trajectory tracking control

can be reduced while satisfying the vehicle kinematics and dynamics constraints. Based on model predictive control, Tong Wu et al. [8] developed a trajectory-tracking control algorithm by defining the error based on the curvature of the reference path for a semi-trailer train. The method significantly reduces the tracking error of the vehicle at the junction of a straight line and a circular arc. Zhituo Ni et al. [9] investigated the active steering technology of a trailer based on a linear quadratic regulator. The dynamic steering controller was designed using the LQR method based on linear matrix inequalities, and the weight coefficients of the controller were optimized to improve the robustness of the steering control. Using a nonlinear observer, Oskar Ljungqvist et al. [10] improved the accuracy of the trajectory tracking control of a semi-trailer train. Using a steering motor at the articulation between a tractor and a semi-trailer, Zhiyuan Liu et al. [11] designed an active articulated structure. A model predictive control algorithm is used to construct an attitude controller, and a sliding film control strategy is used to build a dynamic controller. The maneuverability, performance, and driving stability of the semi-trailer train have improved. Zhenyuan Bai et al. [12], with the tractor and semi-trailer's yawing angular rate as the control objective, proposed a lateral followability control strategy. It can improve the lateral followability of semi-trailer trains, prevent the vehicle from skidding and instability, and improve driving safety. Mehdi Abroshan et al. [13] designed a differential braking control strategy based on a model predictive control algorithm based on an affine tire force model. The control can effectively prevent the occurrence of two unstable phenomena: folding and serpentine traveling. Guang Xia et al. [14] for the problem that stability and feasibility cannot be satisfied simultaneously in the reversing control of semi-trailer trains. By analyzing the coupling relationship between the articulation angle when reversing and the semi-trailer swing angle and other parameters, the feasible domain of the articulation angle when flipping the semi-trailer is determined, and the trajectory tracking control is carried out by adopting fuzzy control with the variable theory domain. The control strategy can prevent the semi-trailer train from folding during the reversing process.

Most existing studies focus on improving the trajectory tracking control accuracy or vehicle driving performance of semi-trailer trains. In this paper, we hope to improve the driving performance of the vehicle without degrading the trajectory tracking accuracy. The differential braking control strategy is formulated on the basis of adopting MPC (Model predictive control) for trajectory tracking control of self-driving semi-trailer trains, and the differential braking is utilized to generate additional yawing moments to improve the driving performance of the vehicle. Differential braking control strategies are designed for low-speed and high-speed operating conditions, respectively, and (Proportional Integral Derivative) and Fuzzy PID algorithms solve the additional yawing moment. To ensure the trajectory tracking control accuracy at the same time, low-speed conditions are needed to improve vehicle mobility, and high-speed conditions are needed to improve the stability of the vehicle.

The trajectory tracking control strategy proposed in this paper is shown in Figure 1.

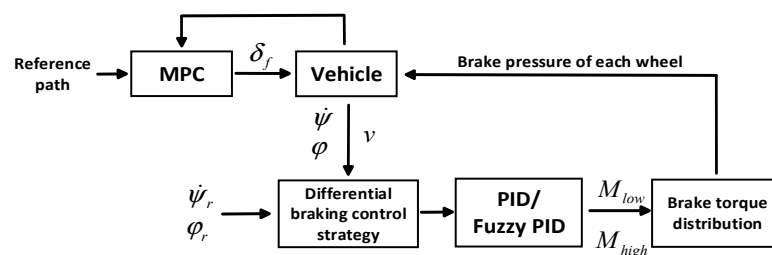


Figure 1. Vehicle trajectory tracking control principle, where δ_f is the front wheel turning angle of the tractor, v is the vehicle speed, $\dot{\psi}_r$ is the desired yawing angular rate of the tractor, $\dot{\psi}$ is the actual yawing angular rate of the tractor, φ_r is the desired articulation angle, φ is the actual articulation angle, M_{low} is the target additional yaw moment at low speed, and M_{high} is the target additional yaw moment at high speed.

2. Vehicle Dynamic Model

A semi-trailer train consists of two parts, a tractor and a semi-trailer, which are connected by articulation, where the tractor is usually two axles and the semi-trailer is usually three axles [15]. The following assumptions were made in modeling the semi-trailer train: (1) The three axles of the trailer are equivalent to a single axle (equivalent to an intermediate axle), and the left and right wheels on the same axle are equal to one wheel. (2) Only the rear wheels of the tractor are driving wheels. (3) It is assumed that the sideways and pitching motions of the semi-trailer train while traveling are so small that they can be ignored. (4) There is a linear relationship between the lateral yawing force and the lateral yawing angle of all wheels. (5) The effect of vertical load variation on wheel-side deflection characteristics is not considered.

A semi-trailer train dynamics model is established based on the above assumptions, as shown in Figure 2.

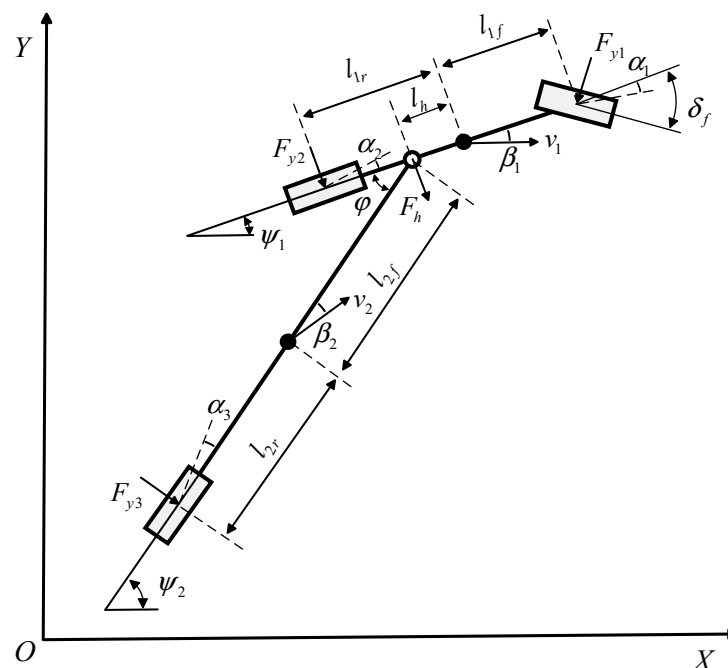


Figure 2. Vehicle kinematic model, where l_{1f} is the distance from the center of mass of the tractor to the front axle. l_{1r} is the distance from the center of mass of the tractor to the rear axle. l_h is the distance from the center of mass of the tractor to the point of articulation. l_{2f} is the distance from the center of mass of the semi-trailer to the articulation point. l_{2r} is the distance between the center of mass of the semi-trailer and the intermediate axle of the semi-trailer. δ_f is the front wheel angle of the tractor. φ is the articulation angle between the tractor and the semi-trailer. ψ_1 and ψ_2 are the yaw angles of the tractor and semi-trailer, respectively. β_1 and β_2 are the center-of-mass lateral deflection angles of the tractor and semi-trailer, respectively. α_1 , α_2 and α_3 are the front wheel sideslip angle of the tractor, the rear wheel sideslip angle of the tractor, and the rear wheel side deflection angle of the semi-trailer, respectively. F_{y1} , F_{y2} and F_{y3} are the lateral reaction force of the ground on the front wheels of the tractor, the lateral reaction force of the ground on the rear wheels of the tractor, and the lateral reaction force of the ground on the rear wheels of the semi-trailer, respectively. F_h is the force between the tractor and the semi-trailer at the articulation point. k_1 , k_2 and k_3 are the tractor front tire side deflection stiffness, tractor rear tire side deflection stiffness, and semi-trailer rear tire side deflection stiffness, respectively.

The tractor and the semi-trailer are simplified as rods with masses m_1 and m_2 respectively. The effects of aerodynamics and road gradients are neglected. According to

Newton’s laws of mechanics, the dynamic equations of the tractor can be obtained as follows [16]:

$$\begin{cases} m_1 v_1 (\dot{\psi}_1 - \dot{\beta}) = F_{y1} \cos \delta_f + F_{y2} + F_h \\ I_{1z} \ddot{\psi}_1 = F_{y1} l_{1f} - F_{y2} l_{2r} - F_h l_h \end{cases} \quad (1)$$

where v_1 is the speed at the center of mass of the tractor, $\dot{\beta}_1$ and $\dot{\psi}_1$ are the lateral yaw rate and yaw rate of the center of mass of the tractor, respectively. I_{1z} is the moment of inertia of the tractor about the Z axis. $\ddot{\psi}_1$ is the yaw angular acceleration of the tractor.

According to Newton’s laws of mechanics, the dynamic equations of the semi-trailer can be obtained as:

$$\begin{cases} m_2 v_2 (\dot{\psi}_2 - \dot{\beta}_2) = F_{y3} + F_h \cos \varphi \\ I_{2z} \ddot{\psi}_2 = F_h \cos \varphi l_{2f} - F_{y3} l_{2r} \end{cases} \quad (2)$$

where v_2 is the speed at the center of mass of the tractor, $\dot{\beta}_2$ and $\dot{\psi}_2$ are the sideslip angle rate and yaw angle rate of the center of mass of the semi-trailer, respectively, I_{2z} is the moment of inertia of the semi-trailer about the Z axis, $\ddot{\psi}_2$ is the yaw angular acceleration of the semi-trailer.

Based on the previous assumptions, all the tires of the semi-trailer train always work in the linear region. Using the linear tire model, the front and rear axle tire forces of the tractor and the rear axle tire force of the semi-trailer are:

$$\begin{cases} F_{y1} = k_1 (\beta_1 + l_{1f} \dot{\psi}_1 / v_1 - \delta_f) \\ F_{y2} = k_2 (\beta_1 - l_{1r} \dot{\psi}_1 / v_1) \\ F_{y3} = k_3 (\beta_2 - l_{2r} \dot{\psi}_2 / v_2) \end{cases} \quad (3)$$

The kinematic constraints between the tractor and the semi-trailer during the travel of the semi-trailer train are:

$$\dot{\beta}_1 - \dot{\beta}_2 - \frac{l_h}{v_1} \ddot{\psi}_1 - \frac{l_{2r}}{v_1} \ddot{\psi}_2 + \dot{\psi}_1 - \dot{\psi}_2 = 0 \quad (4)$$

According to Equations (1), (2), and (4), the state-space equation of the semi-trailer train can be expressed as follows:

$$\begin{cases} \dot{x} = Ax + BU \\ y = Cx \end{cases} \quad (5)$$

where $x = [y_2 \ \beta_1 \ \dot{\psi}_1 \ \beta_2 \ \dot{\psi}_2]^T$, $U = [\delta_f]^T$, x is the vehicle state profile. U is the vehicle control profile.

Matrix A , B , and C are, respectively:

$$N = \begin{bmatrix} 0 & 0 & 0 & 0 & 0 \\ 0 & m_1 v_1 l_3 & I_{1z} & 0 & 0 \\ 0 & m_1 v_1 & 0 & m_2 v_2 & 0 \\ 0 & 0 & 0 & m_2 v_2 l_5 & -I_{2z} \\ 0 & -1 & \frac{l_h}{v_1} & 1 & \frac{l_{2f}}{v_2} \end{bmatrix}, A = N^{-1} \begin{bmatrix} 0 & 0 & 0 & v_2 & 0 \\ 0 & a_{22} & a_{23} & 0 & 0 \\ 0 & k_1 + k_2 & a_{33} & k_3 & a_{35} \\ 0 & 0 & 0 & a_{44} & a_{45} \\ 0 & 0 & 1 & 0 & -1 \end{bmatrix},$$

$$a_{22} = (l_h + l_{1f})k_1 + (l_h - l_{1r})k_2, a_{23} = \frac{l_{1f}(l_h + l_{1f})k_1 - l_{1r}(l_h - l_{1r})k_2}{v_1} - m_1 v_1 l_h, a_{33} = \frac{l_{1f}k_1 - l_{1r}k_2}{v_1} - m_1 v_1,$$

$$a_{35} = -\frac{l_{2r}k_3}{v_2} - m_2 v_2, a_{44} = (l_{2f} + l_{2r})k_3, a_{45} = -\frac{l_{2r}(l_{2f} + l_{2r})k_3}{v_2} - m_2 v_2 l_{2f},$$

$$B = N^{-1} \begin{bmatrix} 0 & - (l_h + l_{1f})k_1 & -k_1 & 0 & 0 \end{bmatrix}^T, C = \begin{bmatrix} 1 & 0 & 0 & 0 & 0 \end{bmatrix}$$

Since a computer controls the physical object, the state space equations of the semi-trailer train are written in discrete form for the convenience of the controller design [16]:

$$\begin{cases} x(k+1) = A_c x(k) + B_c \delta_f(k) \\ y(k) = C_c x(k) \end{cases} \quad (6)$$

where $A_c = e^{AT_s}$, $B_c = \int_0^{T_s} e^{A\tau} d\tau \cdot B$, $C_c = C$, T_s is the sampling time.

3. Trajectory Tracking Control

This paper uses model predictive control theory to design the trajectory tracking algorithm [17]. The model predictive control adopts a rolling optimization strategy, meaning the optimization calculation can be repeated online. It can timely and effectively compensate for tracking errors due to perturbations and other factors, thus improving tracking accuracy.

The principle of MPC trajectory tracking control is shown in Figure 3:

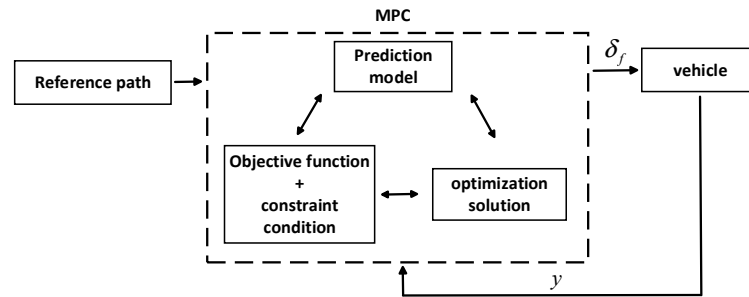


Figure 3. MPC trajectory tracking control principle.

Typical model predictive control consists of three key components: the predictive model, rolling optimization, and feedback correction. The MPC works as shown in Figure 4.

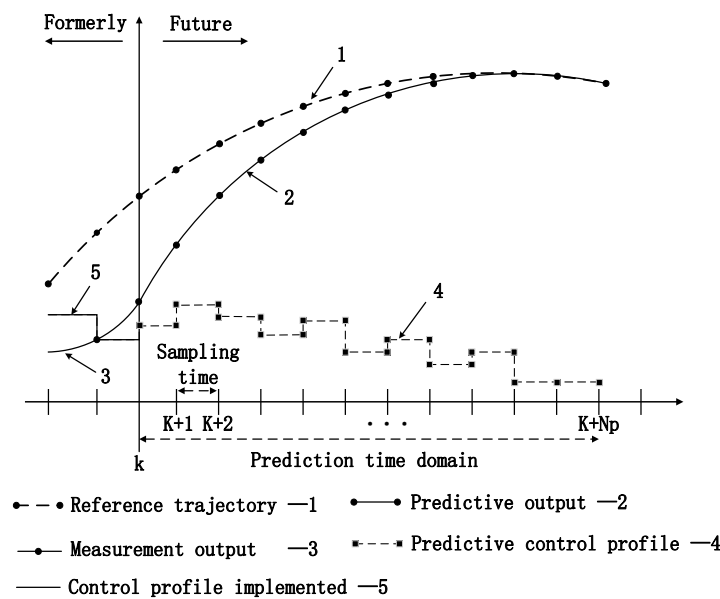


Figure 4. MPC principle.

The controller predicts the output of the system at a future time $[k, k + N_p]$ based on the measured values at the current moment k with the prediction model. N_p is the prediction time domain. A series of optimal control sequences in the control time domain are obtained by solving the problem of minimizing the cost function while satisfying the constraints. The control profiles at the moment k in the control sequence are used as the actual input of the controlled object, which is brought into the system state transfer equation to obtain the state of the system at the moment $k + 1$. The above process is repeated to update the optimization problem based on the new state quantities and then re-solve it, following which a closed-loop control system is obtained.

Using Equation (6) as the prediction model, the predicted output of the system can be expressed as:

$$Y(k + 1|k) = C_x X(k + 1|k) + C_u U(k) \tag{7}$$

$$\text{where } Y(k+1|k) = \begin{bmatrix} y(k+1|k) \\ y(k+2|k) \\ \vdots \\ y(k+P|k) \end{bmatrix}, C_x = \begin{bmatrix} C_c A_c \\ \vdots \\ C_c A_c^N \\ \vdots \\ C_c A_c^P \end{bmatrix}, X(k+1|k) = \begin{bmatrix} x(k+1|k) \\ x(k+2|k) \\ \vdots \\ x(k+P|k) \end{bmatrix},$$

$$U(k) = \begin{bmatrix} \delta_f(k|k) \\ \delta_f(k+1|k) \\ \vdots \\ \delta_f(k+P-1|k) \end{bmatrix}, C_u = \begin{bmatrix} C_c B_c & 0 & \cdots & 0 \\ \vdots & \vdots & \ddots & \vdots \\ C_c A_c^{N-1} B_c & C_c A_c^{N-2} B_c & \cdots & C_c B_c \\ \vdots & \vdots & \ddots & \vdots \\ C_c A_c^{P-1} B_c & C_c A_c^{P-2} B_c & \cdots & \sum_{i=1}^{P-N+1} C_c A_c^i B_c \end{bmatrix}$$

The objective function is a vital part of the model’s predictive control. The objective function is designed to ensure that the planned path can be tracked accurately and, at the same time, to ensure the stability of the vehicle traveling during the tracking process [18].

The trace item of the reference path is written as:

$$J_1 = \|Y(k+1|k) - Y_r(k)\|^2 \tag{8}$$

where $Y_r(k) = [y_r(k+1), y_r(k+2), \dots, y_r(k+P)]^T$, represents a series of discrete trace points on the reference path in the prediction time domain.

To maintain the stability of the vehicle traveling during trajectory tracking control, the vehicle control action should change as smoothly as possible. To achieve such goals, minimize the following cost function:

$$J_2 = \|U(k)\|^2 \tag{9}$$

The control objective of the trajectory tracking control algorithm is to satisfy the trajectory tracking accuracy while keeping the change frequency of the vehicle control action as small as possible. By introducing a matrix of weight coefficients to weigh the relationship between J_1 and J_2 , the objective function of the controller can be written as:

$$J = \| [W_y Y(k+1|k) - Y_r(k)] \|_2 + \| W_u U(k) \|^2 \tag{10}$$

where W_y and W_u are the weight coefficient matrices of the state profiles and control profiles.

Considering the inherent characteristics of the vehicle’s mechanical system, the amount of vehicle control and control increments should satisfy the following constraints:

$$\begin{cases} u_{\min} \leq u(k+i) \leq u_{\max} \\ \Delta u_{\min} \leq \Delta u(k+i) \leq \Delta u_{\max} \end{cases} \tag{11}$$

where $\Delta u(k+1) = u(k+1) - u(k)$, u_{\min} and u_{\max} are the minimum and maximum values of the control profiles, respectively. Δu_{\min} and Δu_{\max} are the minimum and maximum values of the control increment, respectively. The control profiles here are mainly the front wheel angle δ_f of the tractor.

Finally, the trajectory tracking control problem based on model predictive control theory is transformed into solving the optimization problem with constraints. The optimal

front wheel angle of a semi-trailer train can be obtained by solving the optimization problem with constraints.

$$\begin{aligned}
 & \text{Minimize} = J(X(k), U(k)) \\
 & \quad U(k) \\
 & \text{subject to} \\
 & \quad u_{\min} \leq u(k+i) \leq u_{\max} \\
 & \quad \Delta u_{\min} \leq \Delta u(k+i) \leq \Delta u_{\max}
 \end{aligned} \tag{12}$$

4. Differential Brake Control

Differential braking improves a vehicle’s driving performance by providing different braking forces to different wheels during the vehicle’s traveling process so that the car generates additional yaw moments [19]. Compared with technologies such as active rear-axle steering, differential braking does not require other hardware and can be realized by using mature brake control technology to achieve precise distribution of braking force to the wheels, which is low-cost and easy to accomplish [20,21]. The implementation of differential brake control requires the use of an accurate vehicle model. Based on the vehicle dynamics model in Section 2, the additional yaw moment generated by differential braking is added. The yawing moment and the front wheel angle of the tractor are jointly used as system inputs to obtain the semi-trailer train dynamics model, considering the additional yaw moment. As shown in Figure 5:

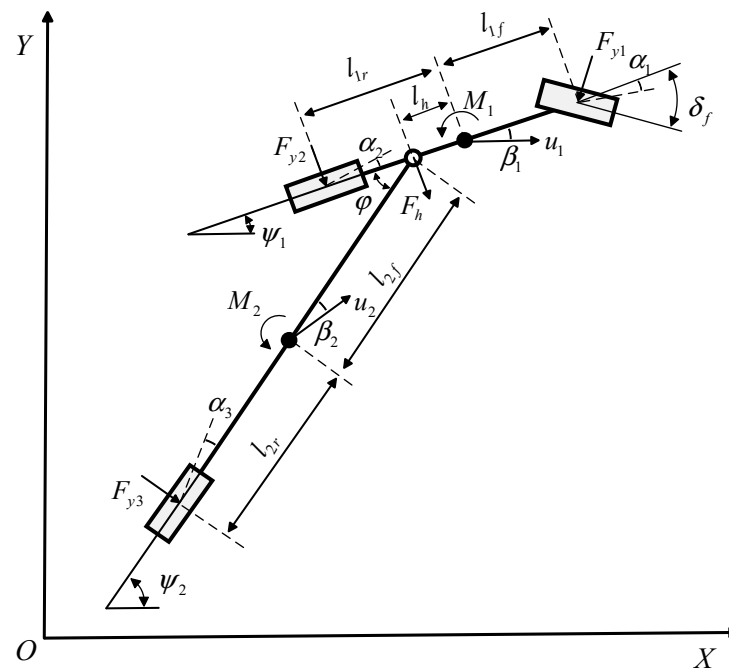


Figure 5. Vehicle dynamics model considering additional yaw moment.

Based on Equation (5), the state-space equation of the semi-trailer train considering the additional yaw moment is obtained as (Moment is equal to moment of inertia times angular acceleration):

$$\begin{cases} \dot{x} = Ax + BU + B_1M_z \\ y = Cx \end{cases} \tag{13}$$

where $B_1 = \begin{bmatrix} 0 & 0 & \frac{1}{I_{1z}} & 0 & 0 \\ 0 & 0 & 0 & 0 & \frac{1}{I_{2z}} \end{bmatrix}^T$, $M_z = [M_{tractor} \quad M_{trailer}]^T$, M_z is the total additional yaw moment generated by differential braking of semi-trailer train, $M_{tractor}$ is the additional yaw moment of target generated by the differential braking of tractor, $M_{trailer}$ is the target additional yaw moment generated by differential braking of the semi-trailer, I_{1z} is the

moment of inertia of the tractor about the Z axis, I_{2z} is the moment of inertia of the semi-trailer about the Z axis.

In this paper, two control strategies are designed for the different needs of vehicle driving performance under the two driving conditions of low speed (Initial velocity ≤ 30 km/h) and high speed (Initial velocity ≥ 70 km/h) of semi-trailer trains. It is hoped to improve the vehicle's maneuverability at low-speed and stability at high-speed. The differential braking control strategy is shown in Figure 6.

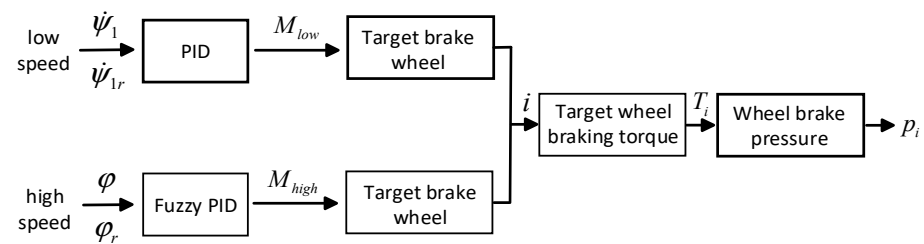


Figure 6. Differential braking control strategy.

4.1. Low-Speed Differential Brake Control

During the turning process of the semi-trailer train, the two parts of the car body can make a certain angle with each other, and there is an articulation angle [22]. The articulation angle of a semi-trailer train is defined as the angle between the tractor's longitudinal axis and the semi-trailer's longitudinal axis and is indicated by the symbol. The presence of an articulation angle makes the turning radius of the outer contour of the body smaller and that of the inner shape larger when the semi-trailer train is turned. Compared to a single car of the same size, a semi-trailer train sweeps a smaller area of the road during a turn and, therefore, has good maneuverability. Under the premise of ensuring that the semi-trailer train does not fold, appropriately increasing the articulation angle can reduce the turning radius of the semi-trailer train, which is conducive to improving the passability of the semi-trailer train in the narrow channel. Therefore, a control strategy to increase the articulation angle using differential braking is developed for low-speed conditions.

4.1.1. Additional Yaw Moment

The semi-trailer train's whole vehicle driving force comes from the tractor; the semi-trailer in the tractor towing under the driving semi-trailer's presence on the tractor is equivalent to the tractor in the rear of the tractor imposing a driving resistance. Compared with the tractor driving alone, the yaw rate of the tractor-towing semi-trailer will be inhibited. A significant yaw rate contributes to a large articulation angle. In this paper, the yaw rate of the tractor is taken as the reference yaw rate, and the PID control algorithm is designed to make the actual yaw rate tend to the reference yaw rate, and the additional yaw moment under the low-speed condition is obtained.

According to the vehicle model, when the tractor is driving alone, the ideal yaw rate of the tractor is calculated as follows:

$$\dot{\psi}'_1 = \frac{v_1/l}{1 + Kv_1^2} \delta_f \tag{14}$$

where $l = l_{1f} + l_{1r}$, $K = \frac{m}{l^2} (\frac{l_{1f}}{k_2} - \frac{l_{1r}}{k_1})$, is the stability factor, v_1 is the speed of the tractor. k_1 and k_2 are the lateral stiffness of the front and rear axles of the vehicle, respectively.

The road adhesion conditions limit the ideal yaw rate [23], and the lateral acceleration must meet the constraints under the tire adhesion limit:

$$|a_y| = \mu \cdot g \tag{15}$$

where a_y is the lateral acceleration of the tractor, μ is the road adhesion coefficient, and g is the acceleration of gravity.

The maximum value of the yaw rate of the pendulum is given for a low-adhesion road surface:

$$\dot{\psi}_{1\max} = \frac{\mu \cdot g}{v_1} \quad (16)$$

Considering driving on low adhesion road surfaces $\dot{\psi}_{1\max} < \dot{\psi}'_1$ and driving on high adhesion road surfaces $\dot{\psi}'_1 > \dot{\psi}_{1\max}$, in order to meet different road conditions, the ideal yaw rate is:

$$\dot{\psi}_{1r} = \min\left\{\left|\dot{\psi}'_1\right|, \left|\dot{\psi}_{1\max}\right|\right\} \cdot \text{sgn}(\delta_f) \quad (17)$$

For low-speed conditions, the PID algorithm solves the target additional yaw moment generated by the differential braking of the semi-trailer train. The control objective of the PID is to eliminate the deviation, which is defined here as the difference between the ideal yawing rate of the tractor and the actual yawing rate.

$$e(t) = \dot{\psi}_1 - \dot{\psi}_{1r} \quad (18)$$

The control profile for eliminating the deviation is the target additional yaw moment. The solution of the additional yaw moment includes three parts: proportion, integral, and differential. The solution formula is as follows:

$$M_{low}(t) = K_p e(t) + K_i \int_0^t e(t) dt + K_d \frac{de(t)}{dt} \quad (19)$$

where $K_i = \frac{K_p}{T_i}$, $K_d = K_p T_d$, K_p is the scale factor, T_i is the integral time constant, T_d is the differential time constant, M_{low} is the additional yaw moment of a semi-trailer train under low-speed conditions.

When the semi-trailer train is running, the semi-trailer is dragged by the tractor. If the tractor and the semi-trailer are braking at the same time, in that case, the drag force of the semi-trailer on the tractor will increase, the speed will decrease significantly, and it is easy to cause the vehicle to stop when driving at a low rate. If only the tractor is braked, there is a tendency for the tractor's yawing angle to increase under the impetus of the semi-trailer's inertia force, which is conducive to increasing the articulation angle and is in line with the control objective of differential braking under low-speed operating conditions. Therefore, only differential braking is applied to the tractor at low speed. M_{low} is the additional yaw moment generated by the differential braking of the tractor.

PID control principle at low-speed is shown in Figure 7:

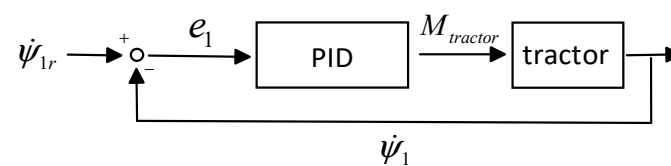


Figure 7. PID control principle.

4.1.2. Target Brake Wheel Decision

The target additional yaw moment of the tractor is obtained by calculating the upper control algorithm of the vehicle. The lower control algorithm performs differential braking on the wheel and realizes the additional yaw moment of the tractor [24]. To ensure the driving stability of the tractor when braking, the braking force is applied to the front and rear wheels of the tractor simultaneously. The target braking wheel of the tractor is determined by comparing the expected yaw response with the actual yaw response.

Taking the process of a right turn and correction of the semi-truck train in single-shift condition as an example, the decision-making method of the target brake wheel is as follows: In the process of the right turn, the expected yaw rate and the actual yaw rate are both clockwise, and the predicted yaw rate is greater than the actual yaw rate. The actual

yaw rate should be compensated for by the additional clockwise yaw moment generated by differential braking. The right wheel of the tractor should be braked. In the correction process, the expected yaw rate and the actual yaw rate are both counterclockwise, and the predicted yaw rate is significantly higher than the actual yaw rate. Differential braking should generate an additional yaw moment counterclockwise to compensate for the real yawing moment. At this time, brake the left-side wheel of the tractor. The differential braking control strategy for low-speed conditions is shown in Figure 8.

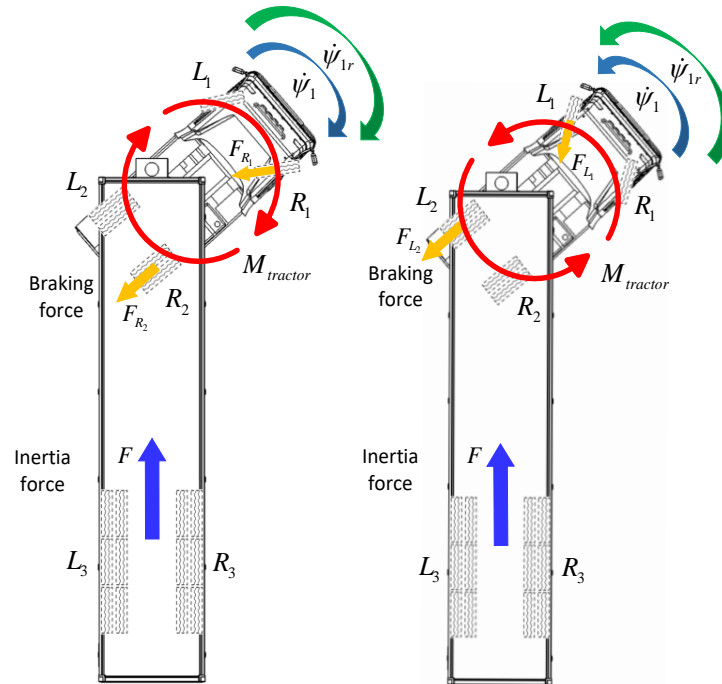


Figure 8. Low-speed differential braking control strategy.

Suppose the yaw rate is negative when it is clockwise and positive when it is counterclockwise. The decision rules for the tractor brake wheel under low-speed conditions are shown in Table 1.

Table 1. Decision rules of brake wheel of low-speed tractor.

| Tractor Expected Yaw Rate Response | Actual Yaw Rate Response of Tractor | Yaw Rate Response Comparison | Tractor Target Brake Wheels |
|------------------------------------|-------------------------------------|----------------------------------|-----------------------------|
| $\dot{\psi}_{1r} > 0$ | $\dot{\psi}_1 > 0$ | $\dot{\psi}_{1r} > \dot{\psi}_1$ | L_1, L_2 |
| $\dot{\psi}_{1r} > 0$ | $\dot{\psi}_1 > 0$ | $\dot{\psi}_{1r} = \dot{\psi}_1$ | - |
| $\dot{\psi}_{1r} > 0$ | $\dot{\psi}_1 > 0$ | $\dot{\psi}_{1r} < \dot{\psi}_1$ | R_1, R_2 |
| $\dot{\psi}_{1r} < 0$ | $\dot{\psi}_1 < 0$ | $\dot{\psi}_{1r} > \dot{\psi}_1$ | R_1, R_2 |
| $\dot{\psi}_{1r} < 0$ | $\dot{\psi}_1 < 0$ | $\dot{\psi}_{1r} = \dot{\psi}_1$ | - |
| $\dot{\psi}_{1r} < 0$ | $\dot{\psi}_1 < 0$ | $\dot{\psi}_{1r} < \dot{\psi}_1$ | L_1, L_2 |
| $\dot{\psi}_{1r} > 0$ | $\dot{\psi}_1 < 0$ | - | L_1, L_2 |
| $\dot{\psi}_{1r} < 0$ | $\dot{\psi}_1 > 0$ | - | R_1, R_2 |
| $\dot{\psi}_{1r} = 0$ | $\dot{\psi}_1 < 0$ | $\dot{\psi}_{1r} < \dot{\psi}_1$ | L_1, L_2 |
| $\dot{\psi}_{1r} = 0$ | $\dot{\psi}_1 > 0$ | $\dot{\psi}_{1r} < \dot{\psi}_1$ | R_1, R_2 |
| $\dot{\psi}_{1r} > 0$ | $\dot{\psi}_1 = 0$ | $\dot{\psi}_{1r} > \dot{\psi}_1$ | L_1, L_2 |
| $\dot{\psi}_{1r} < 0$ | $\dot{\psi}_1 = 0$ | $\dot{\psi}_{1r} > \dot{\psi}_1$ | R_1, R_2 |
| $\dot{\psi}_{1r} = 0$ | $\dot{\psi}_1 = 0$ | $\dot{\psi}_{1r} = \dot{\psi}_1$ | - |

4.2. High-Speed Differential Brake Control

The semi-trailer train travels at a higher speed when turning and changing lanes. Due to the large inertia force, the followability of the semi-trailer to the tractor is poor. The degree of followability is mainly judged by the size of the articulation angle of the semi-trailer train. If the articulation angle is large, it indicates poor follow-ability. If the articulation angle is small, then it demonstrates that the driving follow-ability is good. As a result, when turning and braking, because of the high center of mass position and narrow wheelbase of the semi-trailer train, it is easy to lead to a push-back. This resulted in tire force saturation on the rear axle of the tractor, side slip, and folding of the tractor and semi-trailer caused by the inertial forces of the semi-trailer [25]. Therefore, the differential braking control strategy under high-speed working conditions is to improve the semi-trailer's driving followability for the tractor and then improve the vehicle's driving stability as the control objective [26]. The specific control method is to utilize differential braking to generate additional yaw moment and reduce the articulation angle so that the body of the semi-trailer train can be kept as straight as possible.

4.2.1. Additional Yaw Moment

Take the articulation point of the semi-trailer train as the origin of the coordinate system, and take the longitudinal axis of the tractor as the X-axis to establish the vehicle coordinate system. It is specified that along the positive direction of the X-axis of the vehicle coordinate system, the articulation angle obtained by counterclockwise rotation is positive and the articulation angle obtained by clockwise rotation is negative. The articulation angle is shown in Figure 9.

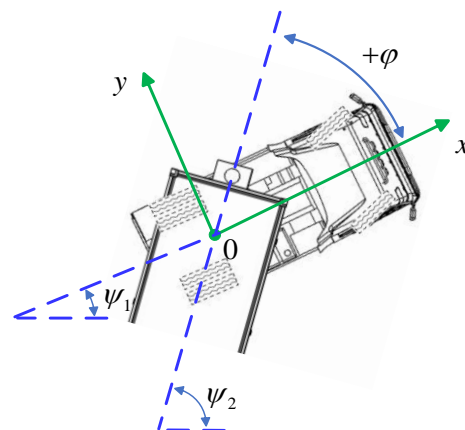


Figure 9. Angle of articulation in tractor coordinate system.

The formula for solving the articulation angle is:

$$\varphi = |\psi_1 - \psi_2| \quad (20)$$

At high speed, a fuzzy PID algorithm solves the target additional yaw moment generated by the differential braking of the semi-trailer train. Fuzzy PID combines the PID algorithm with fuzzy control theory [27], using fuzzy logic and optimizing the parameters of the PID in real-time according to specific fuzzy rules.

The ideal articulation angle for a semi-trailer train under high-speed conditions is 0° , the error here is the actual articulation angle.

$$e_2(t) = \varphi \quad (21)$$

The variation of the error is:

$$e_c(t) = \dot{e}_2(t) \quad (22)$$

The inputs to the fuzzy PID are the error e_2 and the rate of change of the error \dot{e}_c . After the fuzzification process, the fuzzy inference step performs the approximate inference to derive the correction amount $\Delta K_p, \Delta K_i, \Delta K_d$ for K_p, K_i, K_d . Under a certain error and the rate of change of the error, which is then superimposed on the initial PID parameters after clarification [28], the PID parameters are adjusted in real time as the system error and error derivatives change. The principle of fuzzy controllers is shown in Figure 10.

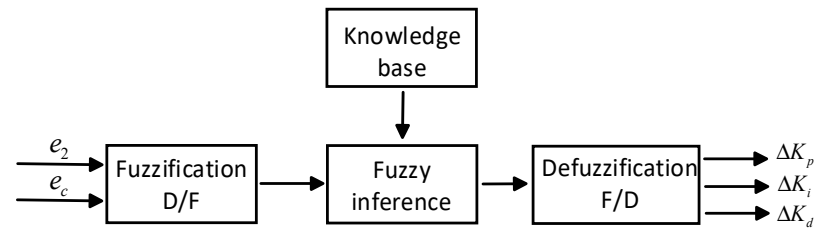


Figure 10. Fuzzy controller principle.

The theoretical domain ranges of both e_2 and e_c are $[-3, 3]$. The theoretical domains of $\Delta K_p, \Delta K_i, \Delta K_d$ are $[-0.3, 0.3], [-0.06, 0.06]$, and $[-0.3, 0.3]$, respectively. The affiliation functions between inputs and outputs are shown in Figure 11.

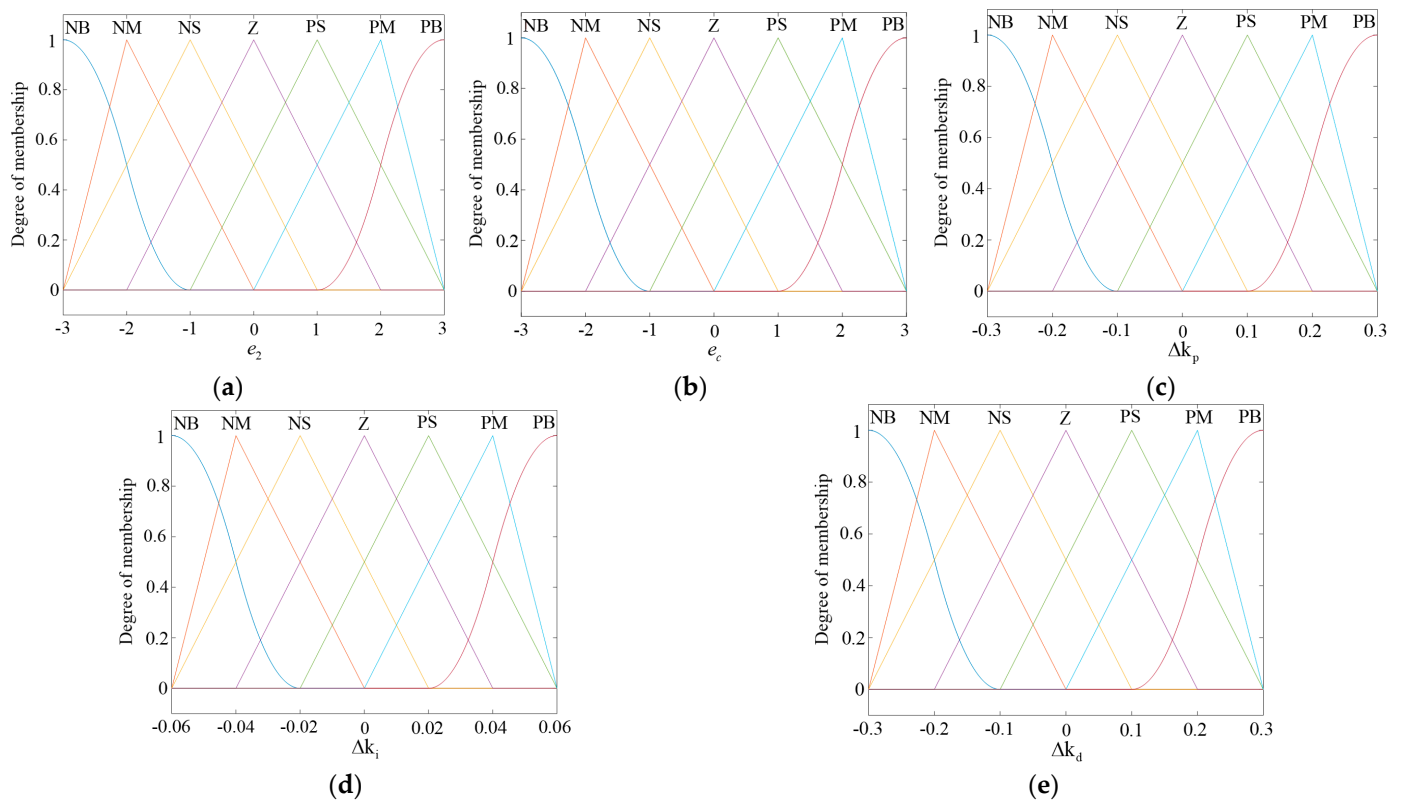


Figure 11. Input and output belong to the membership degree graph. (a) e_2 membership degree; (b) e_c membership degree; (c) ΔK_p membership degree; (d) ΔK_i membership degree; (e) ΔK_d membership degree.

As illustrated in Figure 11, the fuzzy set is divided into {negative big, negative middle, negative small, zero, positive small, positive middle, positive big}, i.e., {NB, NM, NS, Z, PS, PM, PB}. The resulting fuzzy rules are indicated in Tables 2–4.

Table 2. Vague rules for ΔK_p .

| e_2 | e_c | | | | | | |
|-------|-------|----|----|----|----|----|----|
| | NB | NM | NS | Z | PS | PM | PB |
| NB | NB | PB | PM | PM | PS | PS | Z |
| NM | PB | PB | PM | PM | PS | Z | Z |
| NS | PM | PM | PM | PS | Z | NS | NM |
| Z | PM | PS | PS | Z | NS | NM | NM |
| PS | PS | PS | Z | NS | NS | NM | NM |
| PM | Z | Z | NS | NM | NM | NM | NB |
| PB | Z | NS | NS | NM | NM | NB | NB |

Table 3. Vague rules for ΔK_i .

| e_2 | e_c | | | | | | |
|-------|-------|----|----|----|----|----|----|
| | NB | NM | NS | Z | PS | PM | PB |
| NB | NB | NB | NB | NM | NM | Z | Z |
| NM | NB | NB | NM | NM | NS | Z | Z |
| NS | NM | NM | NS | NS | Z | PS | PS |
| Z | NM | NS | NS | Z | PS | PS | PM |
| PS | NS | NS | Z | PS | PS | PM | PM |
| PM | Z | Z | PS | PM | PM | PB | PB |
| PB | Z | Z | PS | PM | PB | PB | PB |

Table 4. Vague rules for ΔK_d .

| e_2 | e_c | | | | | | |
|-------|-------|----|----|----|----|----|----|
| | NB | NM | NS | Z | PS | PM | PB |
| NB | NB | PS | Z | Z | Z | PB | PB |
| NM | NS | NS | NS | NS | Z | NS | PM |
| NS | NB | NB | NM | NS | Z | PS | PM |
| Z | NB | NM | NM | NS | Z | PS | PM |
| PS | NB | NM | NS | NS | Z | PS | PS |
| PM | NM | NS | NS | NS | Z | PS | PS |
| PB | PS | Z | Z | Z | Z | PB | PB |

After determining the affiliation function and formulating the fuzzy logic rules, the fuzzy control surfaces shown in Figure 12 are obtained.

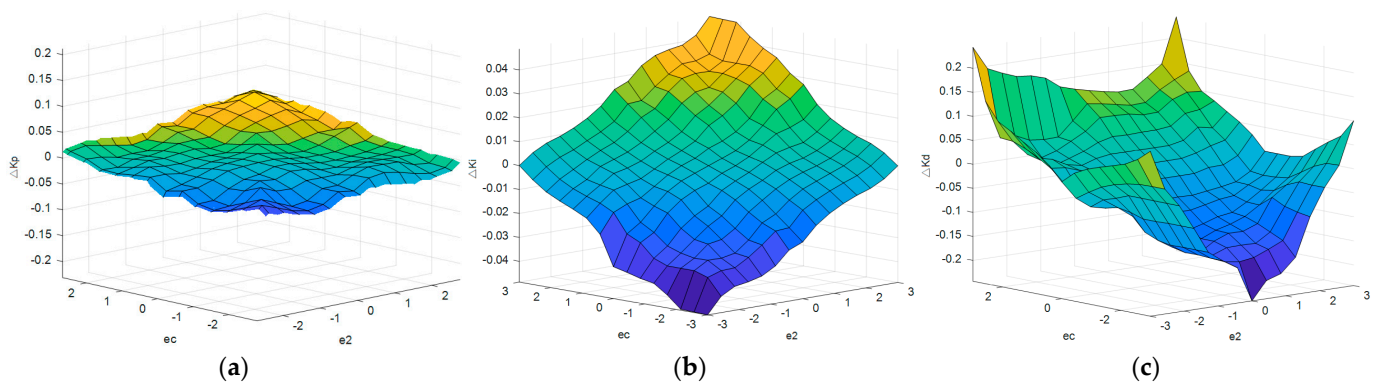


Figure 12. (a), (b), (c) each represent ΔK_p , ΔK_i , ΔK_d fuzzy control surface diagram.

Through the fuzzy control surface of ΔK_p , ΔK_i and ΔK_d three parameters, it can intuitively respond to the fuzzy relationship between input and output and then adjust

the parameters in real-time [29]. The actual parameters of PID are the addition of fixed parameters and corrected parameters.

$$K_p = K'_p + \Delta K_p \tag{23}$$

$$K_i = K'_i + \Delta K_i \tag{24}$$

$$K_d = K'_d + \Delta K_d \tag{25}$$

Under high-speed conditions, the additional yaw moment of the target is calculated by the following formula:

$$M_{high}(t) = K_p e(t) + K_i \int_0^t e(t) dt + K_d \frac{de(t)}{dt} \tag{26}$$

In order to reduce the influence of the inertia force on the driving stability of the tractor, the tractor and the semi-trailer are braking at the same time under high-speed conditions. The additional yaw moment M_{high} must be reasonably distributed between the tractor and the semi-trailer. Considering that the wheel braking force is approximately proportional to its vertical load when the wheel is not locked, the yaw moment of the tractor and semi-trailer is distributed according to the vertical load of each axle.

$$\begin{cases} M_{tractor} + M_{trailer} = M_{high} \\ \frac{M_{tractor}}{M_{trailer}} = \frac{F_{Zf} + F_{Zr}}{F_{Zt}} \end{cases} \tag{27}$$

where $M_{tractor}$ is the additional yaw moment generated by differential braking of a semi-trailer. $M_{tractor}$ is the additional yaw moment generated by the differential braking of the tractor. $M_{trailer}$ is the additional yaw moment generated by the differential braking of a semi-trailer. F_{Zf} , F_{Zr} and F_{Zt} are the dynamic vertical loads of the tractor front axle, rear axle, and semi-trailer rear axle, respectively.

The fuzzy PID control principle is shown in Figure 13:

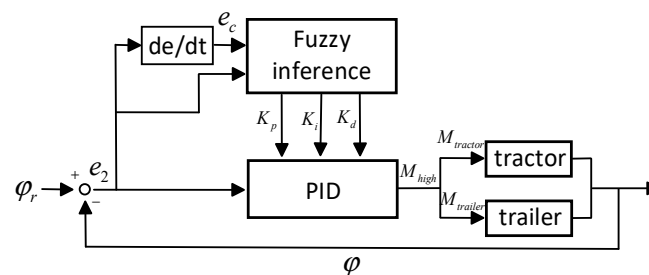


Figure 13. Fuzzy PID control principle.

4.2.2. Target Brake Wheel Decision

Under high-speed conditions, the front and rear wheels of a tractor and the rear wheels of a semi-trailer are involved in differential braking. At this point, the target braking wheel is decided based on whether the semi-trailer train’s articulation angle is positive or negative. Take the case of a positive articulation angle during high-speed steering as follows: In order to reduce the articulated angle of the semi-trailer train, differential braking should be used to produce counterclockwise additional yaw moments of the tractor, and differential braking should be used to produce clockwise additional yaw moments of the semi-trailer. At this time, the tractor’s left side wheel and the semi-trailer’s right side wheel brake simultaneously. The differential braking control strategy for high-speed conditions is shown in Figure 14.

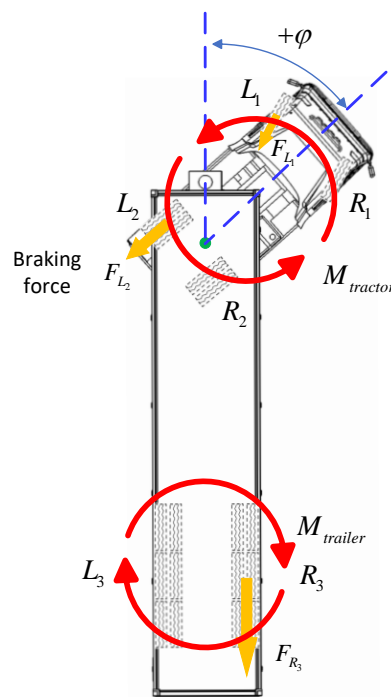


Figure 14. High-speed differential braking control strategy.

According to the articulation angle’s positive or negative value, the decision rules for the brake wheel of a semi-trailer train under high-speed working conditions are shown in Table 5.

Table 5. Decision rules for brake wheel of high-speed semi-trailer trains.

| The Symbol of the Articulation Angle | Tractor Target Brake Wheels | Semi-Trailer Target Brake Wheels |
|--------------------------------------|-----------------------------|----------------------------------|
| $\varphi > 0$ | L_1, L_2 | R_3 |
| $\varphi = 0$ | - | - |
| $\varphi < 0$ | R_1, R_2 | L_3 |

4.3. Target Wheel Brake Pressure

After the wheels for differential braking of semi-trailer trains in different driving modes are determined, the wheel braking torque, and thus the wheel braking pressure, can be determined based on the target additional yaw moments of the tractor and the semi-trailer.

For a tractor, the additional yaw moment needs to be properly distributed between the front and rear axles. Considering that the wheel braking force is approximately proportional to its vertical load when the wheels are not locked and there is axle load transfer in the vehicle under longitudinal and lateral acceleration, to make full use of the road adhesion conditions, the braking torque generated by the front and rear axles of the tractor should meet the following requirements:

$$\begin{cases} T_{1r} + T_{2r} = M_{tractor} \\ \frac{T_{1r}}{T_{2r}} = \frac{F_{Zf}}{F_{Zr}} \end{cases} \quad (28)$$

where T_{1r} and T_{2r} are the target braking torque of the front and rear axles of the tractor, respectively. F_{Zf} and F_{Zr} are the dynamic vertical loads of the front and rear axles of the tractor, respectively.

For semi-trailers, the additional yaw moment is generated by the rear axle of the semi-trailer.

$$T_{3r} = M_{trailer} \quad (29)$$

The front wheels of the tractor are responsible for steering. When the front wheels of the tractor are braked, the front wheel angle of the tractor must be considered when calculating the braking torque. The braking moments of the tractor front axle and unilateral wheels are, respectively, [22]:

$$T_{L_1} = T_{1r} \cdot l_{1wr} / (\sin \delta_f \cdot l_{1f} + \frac{l_{1x}}{2} \cos \delta_f) \quad (30)$$

$$T_{R_1} = T_{1r} \cdot l_{1wr} / (-\sin \delta_f \cdot l_{1f} + \frac{l_{1x}}{2} \cos \delta_f) \quad (31)$$

where T_{1r} is the target braking torque of the front axle of the tractor, l_{1wr} is the front axle tire radius of the tractor, l_{1x} is the front axle wheelbase of the tractor.

The braking torques of the wheels on one side of the rear axle of the tractor are, respectively:

$$T_{L_2} = T_{2r} \cdot l_{2wr} / (\frac{l_{2x}}{2}) \quad (32)$$

$$T_{R_2} = T_{2r} \cdot l_{2wr} / (\frac{l_{2x}}{2}) \quad (33)$$

where T_{2r} is the target braking torque of the rear axle of the tractor, l_{2wr} is the radius of the rear axle tire of the tractor, l_{2x} is the rear axle wheelbase of the tractor.

Semi-trailer rear axle single-side wheel braking torque, respectively:

$$T_{L_3} = T_{3r} \cdot l_{3wr} / (\frac{3 \cdot l_{3x}}{2}) \quad (34)$$

$$T_{R_3} = T_{3r} \cdot l_{3wr} / (\frac{3 \cdot l_{3x}}{2}) \quad (35)$$

where T_{3r} is the target braking torque of the rear axle of the semi-trailer, l_{3wr} is the radius of the rear axle tire of the semi-trailer, l_{3x} is the wheel base of the rear axle of the semi-trailer.

The braking pressure of the target wheel is [30]:

$$p_i = \frac{T_i}{k_i} \quad (36)$$

where $i = L_1, L_2, L_3, R_1, R_2, R_3$ is the wheel code. p_i is the braking pressure of the target wheel and is the main parameter of differential brake control. T_i is the target wheel braking torque. k_i refers to the wheel braking efficiency factor jointly determined by the brake disc friction area, friction factor, etc.

5. Simulation Experiment Verification

In order to verify the effectiveness of the proposed control strategy, a vehicle model of the semi-trailer train was established using TruckSim, and a simulated road scene was constructed. The MPC trajectory tracking control algorithm was first written in MATLAB/Simulink, and then the differential braking control strategy and the distribution rules of braking pressure for each wheel were written on the basis of this algorithm under the working conditions of low speed and high speed. Considering that the semi-trailer vehicle train mainly travels on dry and good asphalt or concrete road surfaces, the road surface adhesion coefficient in the road scenario is set to a fixed value of 0.8 [31]. The main parameters of the semi-trailer train used in the simulation experiments are shown in Table 6. It should be noted in particular that in Figures 15–17, Figures 19–23, and Figures 25–29, the red solid line represents the simulation experimental data when differential braking are applied during trajectory tracking control, and the blue dashed line represents the simulation experimental data when differential braking are not applied. In Figures 18, 24, and 30, FL_1 denotes the left front wheel of the tractor, FL_2 denotes the left rear wheel of the tractor, and FL_3 denotes the left rear wheel of the semi-trailer. FR_1

denotes the right front wheel of the tractor, FR_2 denotes the right rear wheel of the tractor, and FR_3 denotes the right rear wheel of the semi-trailer.

Table 6. Main parameters of semi-trailer train.

| Arguments (units) | Numerical Value |
|--|-----------------|
| Tractor quality (kg) | 5760 |
| Tractor wheelbase (mm) | 3500 |
| Trailer wheelbase (mm) | 2030 |
| Distance from the center of mass of the tractor to the front axle (mm) | 1110 |
| Distance from the center of mass of the tractor to the rear axle (mm) | 2390 |
| The moment of inertia of the tractor about the Z axis (kg/m^2) | 34,823 |
| Tractor steering gear ratio | 25 |
| Semi-trailer quality (kg) | 20,000 |
| Distance from the center of mass of the semi-trailer to the hinge point (mm) | 4000 |
| Semi-trailer wheel gauge (mm) | 1863 |
| The moment of inertia of the semi-trailer about the Z axis (kg/m^2) | 17,999 |

5.1. Validation of Low-Speed Differential Braking Control Strategy

In order to verify the effectiveness of differential braking control under low-speed conditions, the idea of control variables is used to design a right-angle turning scenario to verify the turning radius of a semi-trailer train under a fixed front wheel turning angle. The vehicle turns to the left at a speed of 30 km/h, and the front wheel angle is set to a fixed value of 10° . Plot the trajectory and contour of the vehicle traveling with and without differential brake control. We then plot the variation curve of articulation angle and each wheel braking pressure of a semi-trailer train with and without differential brake control, as shown in Figures 15–18.

It can be seen from the vehicle trajectory maps and the vehicle traveling outline map that the differential braking control strategy reduces the turning radius of the semi-trailer train, which helps the vehicle track the target path with large curvature and improves the vehicle's maneuverability.

It can be seen from the curves of articulation angle that the articulation angle of the semi-truck train under differential braking control is always larger than that without control. With a maximum articulation angle of 20.2° without control and 33.7° with control, the differential brake control increases the maximum articulation angle of the semi-trailer train by about 13.5° . The differential braking control strategy under low-speed conditions increases the articulation angle of the semi-trailer train.

The brake pressure change curves illustrate the magnitude and changes in brake pressure at each tractor wheel during differential brake control.

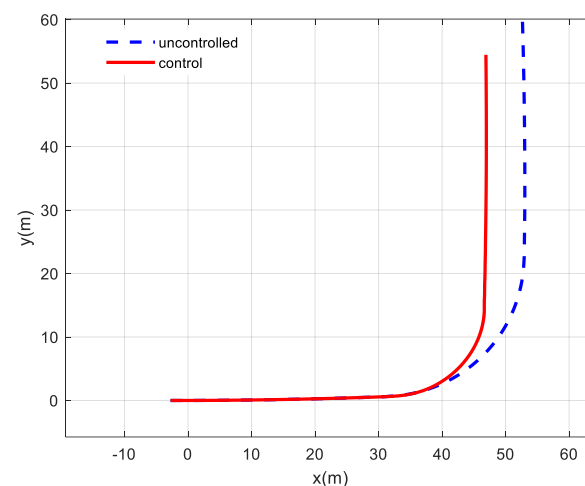


Figure 15. Vehicle trajectory.

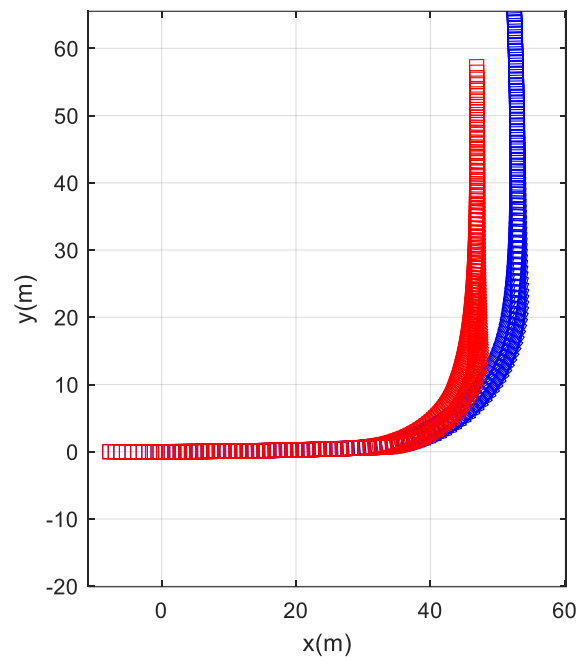


Figure 16. Vehicle contour.

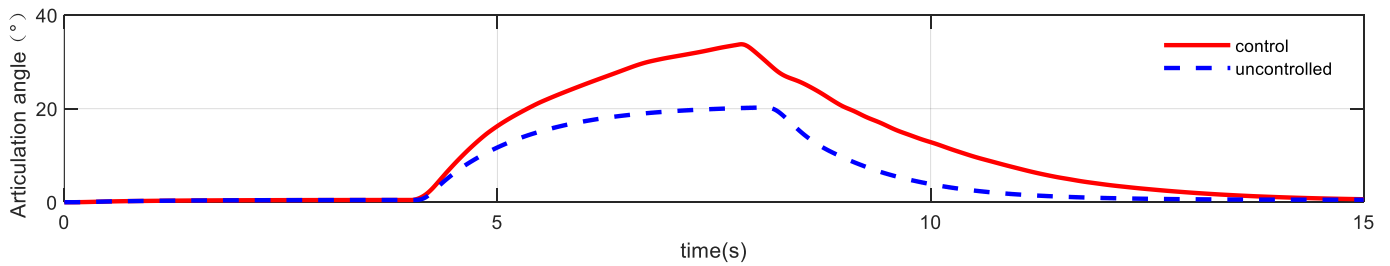


Figure 17. Articulation angle.

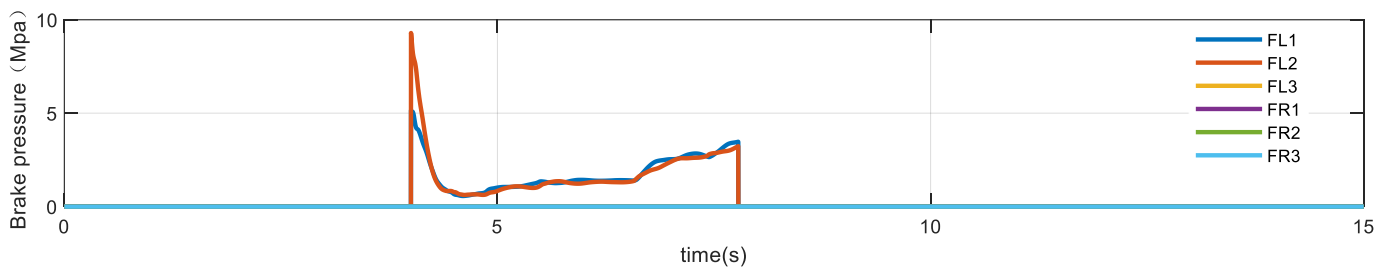


Figure 18. Brake pressure.

5.2. Validation of High-Speed Differential Braking Control Strategy

5.2.1. High-Speed Single-Shift Condition

To verify the effectiveness of the differential braking control strategy for high-speed conditions, simulation experiments are conducted with 80 km/h single-shift conditions as an example. A better understanding is obtained by plotting the trajectory, the articulation angle of the semi-trailer train, the sideslip angle of the tractor, the roll angle of the vehicle, and the change curve of the braking pressure of each wheel with and without differential brake control, as shown in Figures 19–24.

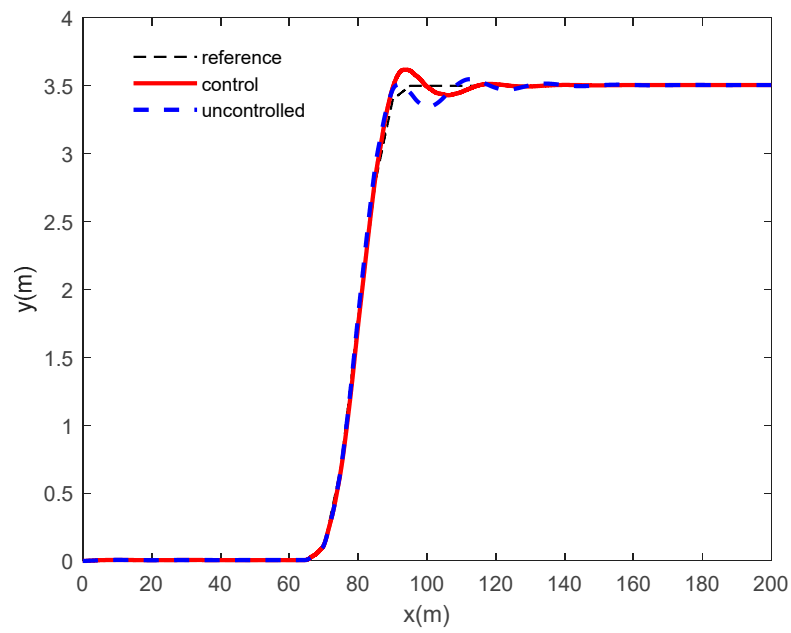


Figure 19. Vehicle trajectory.

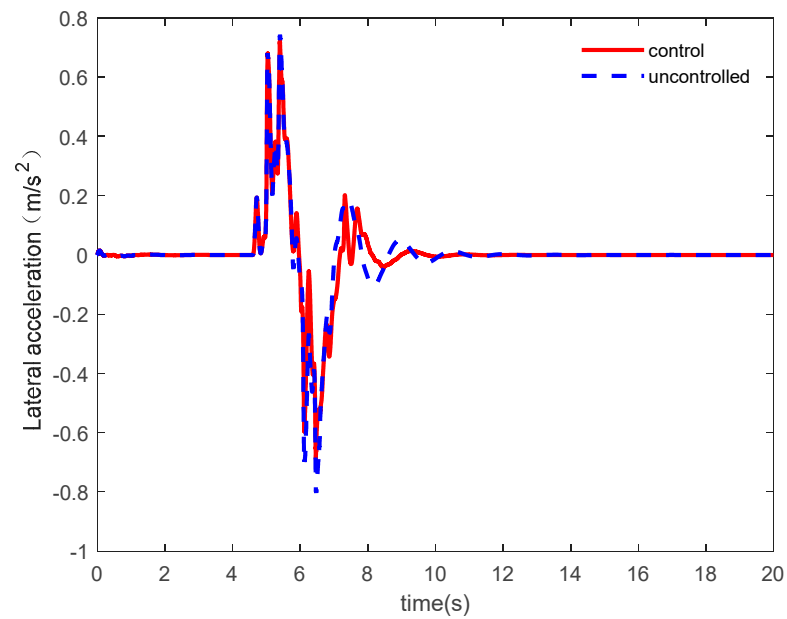


Figure 20. Lateral acceleration.

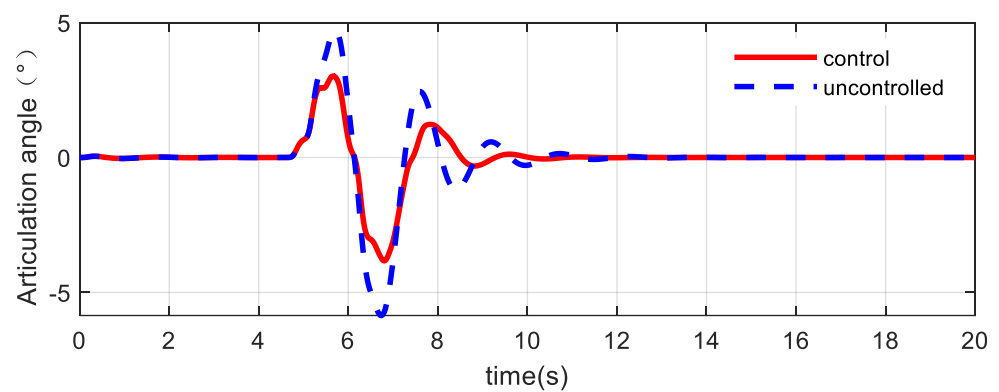


Figure 21. Articulation angle.

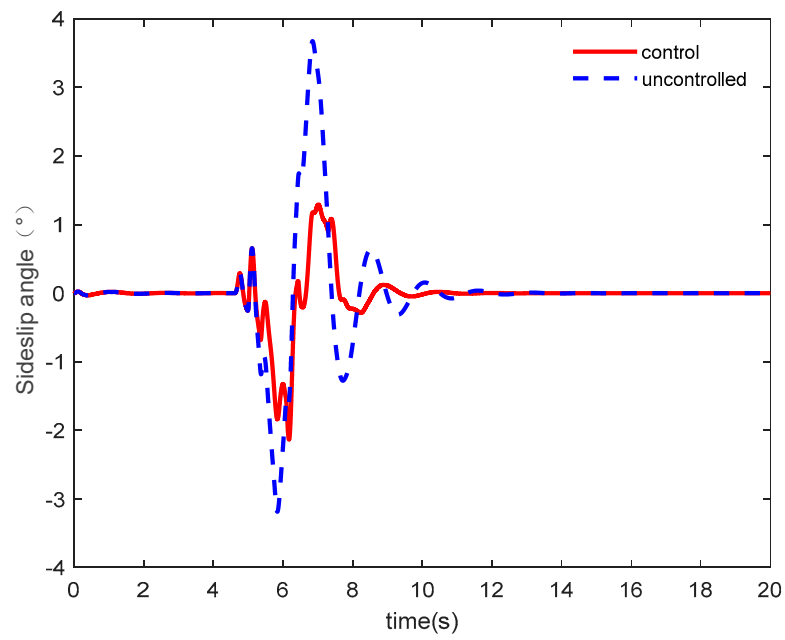


Figure 22. Sideslip angle.

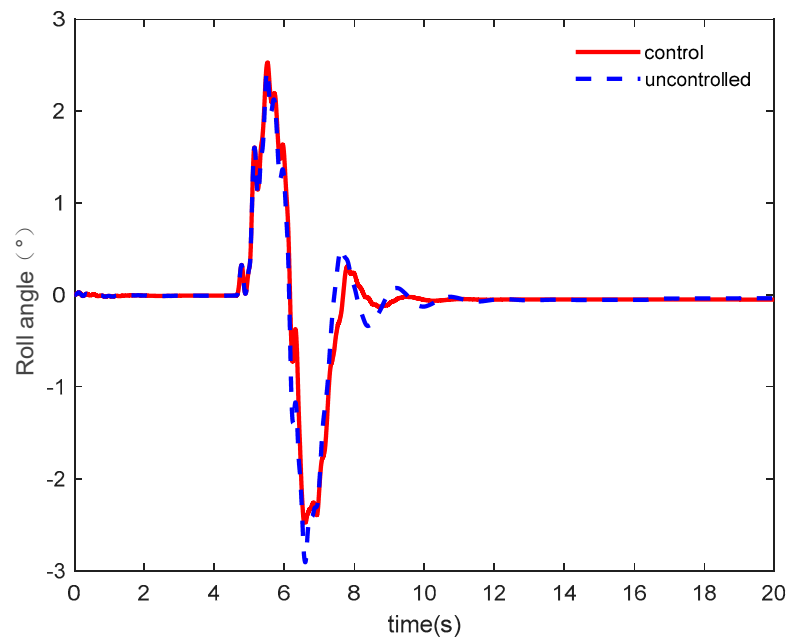


Figure 23. Roll angle.

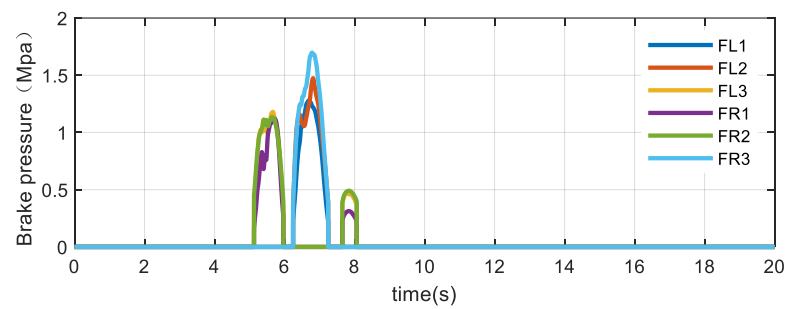


Figure 24. Brake pressure.

From the vehicle trajectory, it can be seen that the error of vehicle trajectory tracking with differential braking control is much smaller than without control. In addition, differential braking control does not reduce the accuracy of trajectory tracking control. Vehicle trajectories with differential brake control show fewer curvature changes than without control, indicating a smoother ride for vehicles with differential braking.

From Equation (15), it is known that under a road surface with an adhesion coefficient of 0.8, the maximum lateral acceleration is 7.84 m/s^2 . As shown in Figure 20, under both conditions with and without differential braking control, the lateral acceleration of the vehicle is much less than the maximum value. This ensures that the vehicle does not skid.

From the change curves of the articulation angle, it can be seen that the articulation angle of the semi-trailer train with differential brake control is always smaller than that of the uncontrolled articulation angle. The maximum articulation angle is -5.85° without control and -3.8° with control. Differential braking control reduces the maximum articulation angle of the vehicle by 2.05° , which improves the following of the semi-trailer to the tractor under high-speed driving conditions.

Semi-trailer train driving through the tractor control to complete, the size of the tractor's sideslip angle will affect the semi-trailer train's maneuvering stability. The tractor sideslip angle change curves show that the tractor sideslip angle under differential brake control is always smaller than the sideslip angle without control. Differential brake control improves the maneuvering stability of semi-trailer trains.

Vehicle roll angle is an important parameter for evaluating vehicle driving stability. From the variation curve of vehicle roll angle, it can be seen that the vehicle roll angle under differential brake control is smaller than without control. Differential brake control can reduce the roll angle and improve the stability of semi-trailer train travelling.

The brake pressure change curves illustrate the magnitude and change of brake pressure on each wheel of a semi-trailer train during differential brake control.

5.2.2. High-Speed Double-Line Shift Condition

As an example, simulation experiments are conducted at 80 km/h in double-shift line conditions. I am plotting the vehicle trajectory with and without differential brake control and the variation curves of the articulation angle of the semi-trailer train, the sideslip angle of the tractor, the roll angle of the vehicle, and wheel braking pressure versus time, as shown in Figures 25–30.

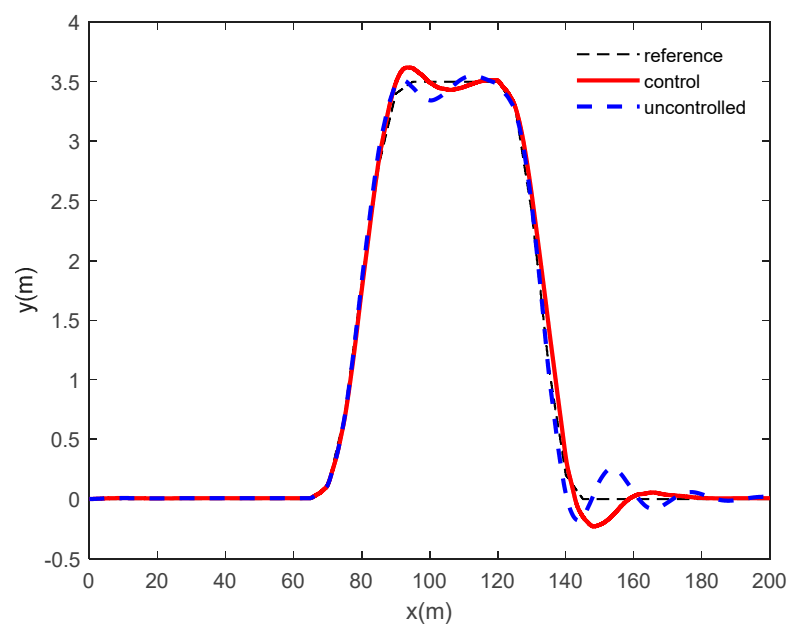


Figure 25. Vehicle trajectory.

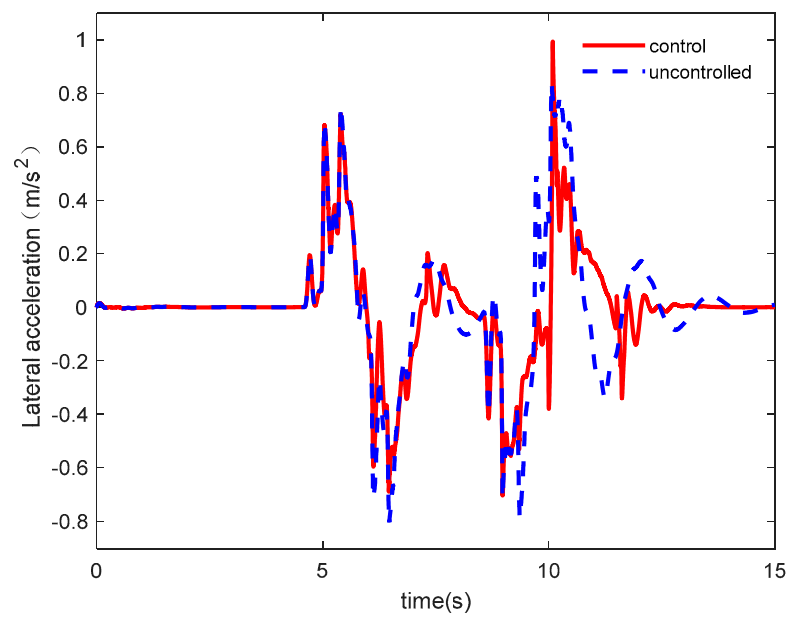


Figure 26. Lateral acceleration.

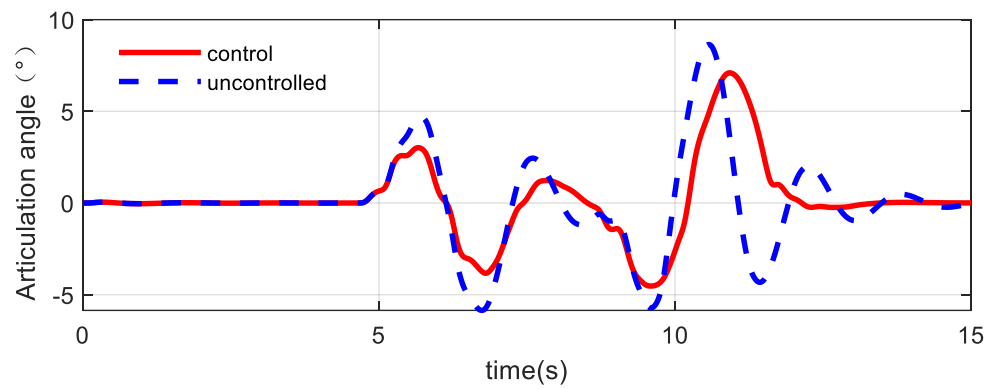


Figure 27. Articulation angle.

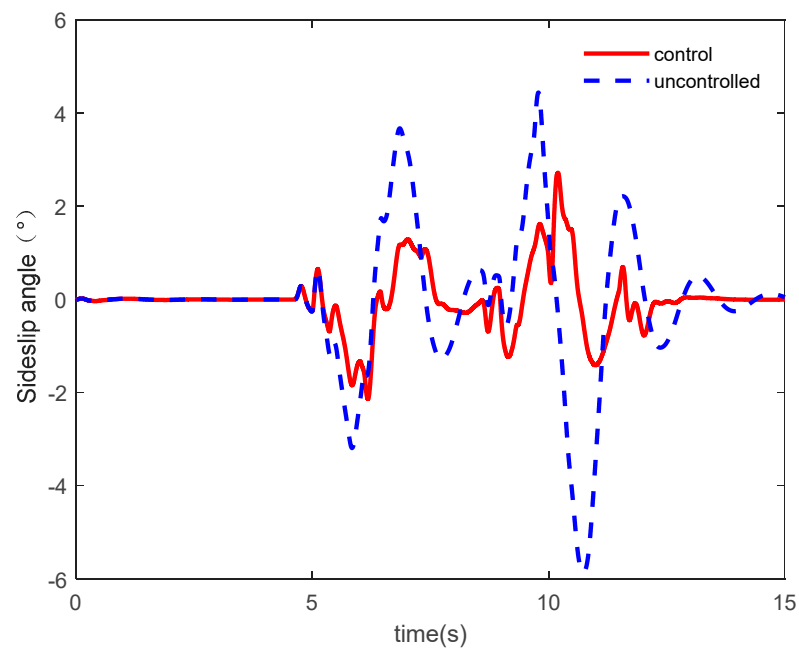


Figure 28. Sideslip angle.

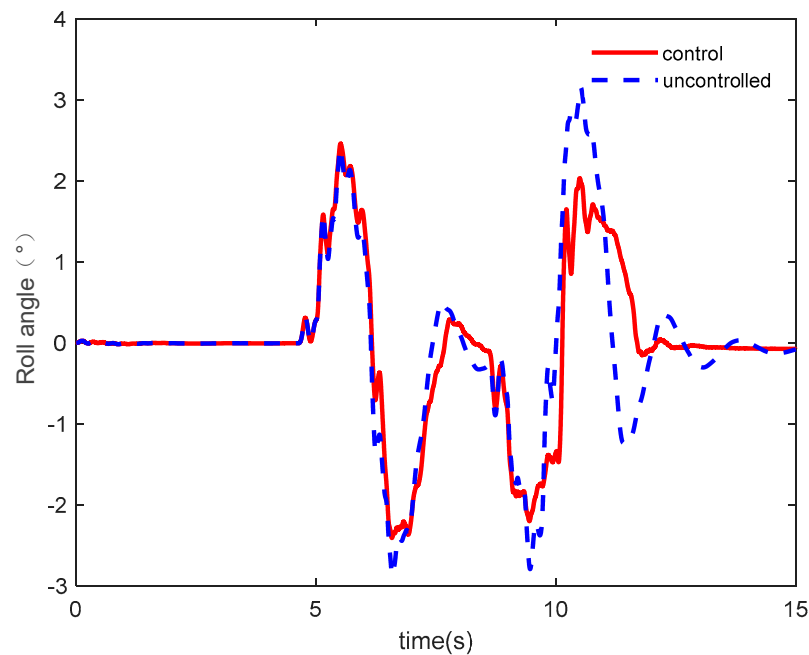


Figure 29. Roll angle.

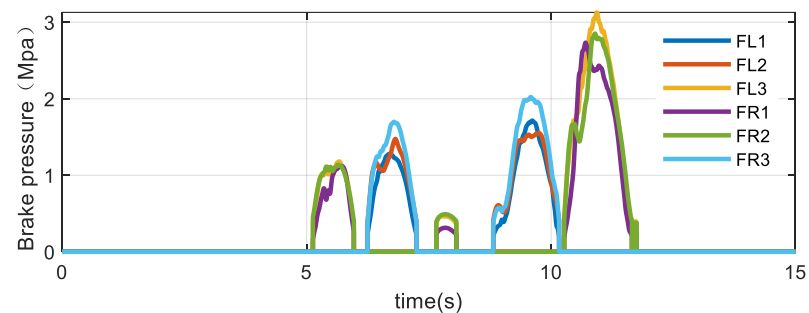


Figure 30. Brake pressure.

From the vehicle trajectory, the vehicle trajectory tracking errors with and without differential brake control are similar, and the differential brake control does not reduce the accuracy of the trajectory tracking control. Under differential brake control, the vehicle trajectory has fewer curvature changes than without control, and the vehicle travels with good stability.

From Equation (15), it is known that under a road surface with an adhesion coefficient of 0.8, the maximum lateral acceleration is 7.84 m/s^2 . As shown in Figure 26, under both conditions with and without differential braking control, the lateral acceleration of the vehicle is much less than the maximum value. This ensures that the vehicle does not skid.

The articulation angle variation curves show that the articulation angle of the semi-trailer train with differential brake control is always smaller than that without control. The maximum articulation angle was reduced by about 1.6° . Consistent with the simulation results of the single moving line condition, the use of differential brake control in the high-speed state improves the semi-trailer's travel following for the tractor.

The tractor sideslip angle change curves show that the tractor sideslip angle under differential brake control is always smaller than the tractor sideslip angle without control, and the peak sideslip angle decreases significantly. Consistent with the conclusions of the single-shift line condition, the differential brake control reduces the sideslip angle of the tractor and improves the maneuvering stability of the semi-trailer train.

From the change curve of vehicle roll angle, it can be seen that the vehicle roll angle under differential brake control is smaller than without control, and the stability of semi-trailer train travel is good.

The curves of brake pressure variation show the magnitude and variation of brake pressure on each wheel in the process of differential brake control.

6. Conclusions

This paper takes the self-driving semi-trailer train as the research object to study its trajectory tracking control problem.

- (1) Differential brake control can effectively improve the driving performance of the vehicle, with the advantages of being low-cost and easy to implement. In this paper, while using MPC for trajectory tracking control of a semi-trailer train, differential braking control is used to improve the driving performance of the vehicle. On the basis of the vehicle dynamics model of the semi-trailer train, the vehicle dynamics model of the semi-trailer train considering the additional yawing moment generated by differential braking is established.
- (2) Under low-speed operating conditions, the desired additional yaw moment is solved by PID using the yaw rate of the tractor when traveling alone as the desired value and the yaw rate of the tractor towing the semi-trailer as the actual value. The target braking wheel is determined by formulating the differential braking control strategy under low-speed working conditions. Simulation experiments show that differential braking control under low-speed working conditions can reduce the turning radius of the semi-trailer train and improve vehicle maneuverability while ensuring trajectory tracking control accuracy.
- (3) Under high-speed working conditions, fuzzy PID is used to solve the desired additional yaw moment with the control objective of reducing the articulation angle of the semi-trailer train. The target braking wheel is determined by formulating the differential braking control strategy under high-speed working conditions. The simulation experiment results show that the differential braking control under high-speed working conditions can reduce the tractor sideslip angle, vehicle roll angle, and articulation angle and improve the stability of the vehicle when driving at high speed.

Currently, there are limitations to this work. In future work, we will consider the effect of the road surface attachment coefficient on the trajectory tracking control process using differential braking control.

Author Contributions: Conceptualization, W.W. and G.L.; methodology, W.W. and S.L.; software, W.W. and G.L.; validation, W.W., G.L. and S.L.; formal analysis, W.W.; investigation, S.L.; resources, G.L. and S.L.; data curation, W.W. and S.L.; writing—original draft preparation, W.W.; writing—review and editing, W.W. and G.L.; visualization, W.W. and G.L.; supervision, G.L.; project administration, G.L.; funding acquisition, G.L. All authors have read and agreed to the published version of the manuscript.

Funding: This work was supported by the General Program of the Natural Science Foundation of Liaoning Province in 2022 (2022-MS-376) and the Natural Science Foundation joint fund project (U22A2043).

Institutional Review Board Statement: Not applicable.

Informed Consent Statement: Not applicable.

Data Availability Statement: The data used to support the findings of this study are available from the corresponding author upon request. The data are not publicly available due to privacy.

Conflicts of Interest: The authors declare no conflict of interest.

References

1. Woźniak, M.; Zielonka, A.; Sikora, A. Driving support by type-2 fuzzy logic control model. *Expert Syst. Appl.* **2022**, *207*, 117798. [[CrossRef](#)]
2. Wei, W.; Ke, Q.; Zielonka, A.; Pleszczyński, M.; Woźniak, M. Vehicle parking navigation based on edge computing with diffusion model and information potential field. *IEEE Trans. Serv. Comput.* **2023**, *16*, 3827–3836. [[CrossRef](#)]
3. Yao, Q.; Tian, Y.; Wang, Q.; Wang, S. Control strategies on path tracking for autonomous vehicle: State of the art and future challenges. *IEEE Access* **2020**, *8*, 161211–161222. [[CrossRef](#)]
4. Liu, X.; Madhusudhanan, A.K.; Cebon, D. Minimum swept-path control for autonomous reversing of a tractor semi-trailer. *IEEE Trans. Veh. Technol.* **2019**, *68*, 4367–4376. [[CrossRef](#)]
5. Zong, C.; Zhu, T.; Wang, C.; Liu, H. Multi-objective stability control algorithm of heavy tractor semi-trailer based on differential braking. *Chin. J. Mech. Eng.* **2012**, *25*, 88–97. [[CrossRef](#)]
6. Leng, Z.; Minor, M.A. Curvature-based ground vehicle control of trailer path following considering sideslip and limited steering actuation. *IEEE Trans. Intell. Transp. Syst.* **2016**, *18*, 332–348. [[CrossRef](#)]
7. Yue, M.; Hou, X.; Gao, R.; Chen, J. Trajectory tracking control for tractor-trailer vehicles: A coordinated control approach. *Nonlinear Dyn.* **2018**, *91*, 1061–1074. [[CrossRef](#)]
8. Wu, T.; Hung, J.Y. Path following for a tractor-trailer system using model predictive control. In Proceedings of the SoutheastCon, 2017, Concord, NC, USA, 30 March–2 April 2017; pp. 1–5. [[CrossRef](#)]
9. Ni, Z.; He, Y. Design and validation of a robust active trailer steering system for multi-trailer articulated heavy vehicles. *Veh. Syst. Dyn.* **2018**, *57*, 1545–1571. [[CrossRef](#)]
10. Ljungqvist, O.; Evestedt, N.; Axehill, D.; Cirillo, M.; Pettersson, H. A Path Planning and Path-following Control Framework for a General 2-trailer with a Car-like Tractor. *J. Field Robot.* **2019**, *36*, 1345–1377. [[CrossRef](#)]
11. Liu, Z.; Yue, M.; Guo, L.; Zhang, Y. Trajectory planning and robust tracking control for a class of active articulated tractor-trailer vehicle with on-axle structure. *Eur. J. Control* **2020**, *54*, 87–98. [[CrossRef](#)]
12. Bai, Z.; Lu, Y.; Li, Y. Method of improving lateral stability by using additional yaw moment of semi-trailer. *Energies* **2020**, *13*, 6317. [[CrossRef](#)]
13. Abroshan, M.; Hajiloo, R.; Hashemi, E.; Khajepour, A. Model predictive-based tractor-trailer stabilisation using differential braking with experimental verification. *Veh. Syst. Dyn.* **2021**, *59*, 1190–1213. [[CrossRef](#)]
14. Xia, G.; Zhao, M.; Tang, X.; Wang, S.; Zhao, L. Linear reversing control of semi-trailer trains based on hitch angle stable and feasible domain. *Control Eng. Pract.* **2020**, *104*, 104625. [[CrossRef](#)]
15. Yu, Z.; Zong, C.; He, L.; Huang, J. Anti-rollover control algorithm for heavy semi-trailer based on LQG. In Proceedings of the 2010 IEEE International Conference on Information and Automation, Harbin, China, 20–23 June 2010; pp. 1593–1596. [[CrossRef](#)]
16. Liu, J.; Zhao, X.; Guo, H.; Chen, H. Tractor Semi-trailer Modeling and Regional Path Tracking Control Strategy. In Proceedings of the 2020 Chinese Automation Congress (CAC), Shanghai, China, 6–8 November 2020; pp. 1961–1966. [[CrossRef](#)]
17. Zhou, Y.; Yang, X.; Mi, C. Dynamic route guidance based on model predictive control. *Comput. Model. Eng. Sci.* **2013**, *92*, 477–491. [[CrossRef](#)]
18. Liu, K.; Hou, Z.; She, Z.; Guo, J. Reentry Attitude Tracking Control for Hypersonic Vehicle with Reaction Control Systems via Improved Model Predictive Control Approach. *Comput. Model. Eng. Sci.* **2020**, *122*, 131–148. [[CrossRef](#)]
19. Zheng, H.; Hu, J.; Ma, S. Research on Simulation and Control of Differential Braking Stability of Tractor Semi-Trailer (No. 2015-01-2842). In Proceedings of the SAE 2015 Commercial Vehicle Engineering Congress, Rosemont, IL, USA, 6–8 October 2015. [[CrossRef](#)]
20. Kim, K.I.; Guan, H.; Wang, B.; Guo, R.; Liang, F. Active steering control strategy for articulated vehicles. *Front. Inf. Technol. Electron. Eng.* **2016**, *17*, 576–586. [[CrossRef](#)]
21. Deng, Z.; Sun, X.; Gao, W. Research on active steering control strategy of articulated heavy vehicles. *Mod. Manuf. Eng.* **2021**, *10*, 17–24. [[CrossRef](#)]
22. Tang, X.; Yan, Y.; Wang, B.; Zhang, L. Adaptive articulation angle preview-based path-following algorithm for tractor-semitrailer using optimal control. *Sensors* **2022**, *22*, 5163. [[CrossRef](#)]
23. Zhang, S.; Li, G.; Wang, L. Trajectory Tracking Control of Driverless Racing Car Under Extreme Conditions. *IEEE Access* **2022**, *10*, 36778–36790. [[CrossRef](#)]
24. Nie, Z. Research on Integrated Control Strategy Combined Differential Braking with Active Rear Axle Steering for Articulated Vehicle. Ph.D. Thesis, University of Jilin, Changchun, China, 2014.
25. Tang, L.; Yan, F.; Zou, B.; Wang, K.; Lv, C. An improved kinematic model predictive control for high-speed path tracking of autonomous vehicles. *IEEE Access* **2020**, *8*, 51400–51413. [[CrossRef](#)]
26. Hou, Y.; Xu, X. High-speed lateral stability and trajectory tracking performance for a tractor-semitrailer with active trailer steering. *PLoS ONE* **2022**, *17*, e0277358. [[CrossRef](#)] [[PubMed](#)]
27. Han, S.Y.; Dong, J.F.; Zhou, J.; Chen, Y.H. Adaptive fuzzy PID control strategy for vehicle active suspension based on road evaluation. *Electronics* **2022**, *11*, 921. [[CrossRef](#)]
28. Zhang, C.; Gao, G.; Zhao, C.; Li, L.; Li, C.; Chen, X. Research on 4WS Agricultural Machine Path Tracking Algorithm Based on Fuzzy Control Pure Tracking Model. *Machines* **2022**, *10*, 597. [[CrossRef](#)]

29. Xue, H.; Zhang, Z.; Wu, M.; Chen, P. Fuzzy controller for autonomous vehicle based on rough sets. *IEEE Access* **2019**, *7*, 147350–147361. [[CrossRef](#)]
30. Ilie, F.; Cristescu, A.C. Tribological Behavior of Friction Materials of a Disk-Brake Pad Braking System Affected by Structural Changes—A Review. *Materials* **2022**, *15*, 4745. [[CrossRef](#)]
31. Janakiraman, B.; Shanmugam, S.; Pérez de Prado, R.; Wozniak, M. 3D road lane classification with improved texture patterns and optimized deep classifier. *Sensors* **2023**, *23*, 5358. [[CrossRef](#)]

Disclaimer/Publisher’s Note: The statements, opinions and data contained in all publications are solely those of the individual author(s) and contributor(s) and not of MDPI and/or the editor(s). MDPI and/or the editor(s) disclaim responsibility for any injury to people or property resulting from any ideas, methods, instructions or products referred to in the content.